17th World Conference on Earthquake Engineering, 17WCEE
Sendai, Japan - September 13th to 18th 2020

Seismic performance enhancement of steel frame building with SMA bracing system

F. Shi[(1)], Y. Zhou[(2)], C. Zhang[(3)], S. H. Kong[(4)] , O. E. Ozbulut[(5)]

[(1)] *Ph. D candidate, School of Civil Engineering, Guangzhou University, shifei1113@126.com*
[(2)] *Professor, School of Civil Engineering, Guangzhou University, zhydxs@163.com*
[(3)] *Associate Professor, School of Civil Engineering, Guangzhou University, zhch2013@gzhu.edu.cn*
[(4)] *Master degree candidate, School of Civil Engineering, Guangzhou University, 904776497@qq.com*
[(5)] *Associate Professor, Department of Civil and Environmental Engineering, University of Virginia, ozbulut@virginia.edu*

Abstract

Shape memory alloys (SMAs) have attracted considerable attentions in civil infrastructure applications with the growing demand for high-performance and more resilient structural systems in last two decades. A number of SMA-based passive control devices have been developed to control seismic response of structures while minimizing residual drifts. However, most of these devices were developed on the basis of wire form of SMAs which possesses low force capacity, which is one of the longstanding impediments for the practical application of SMAs in civil infrastructure. Recently, large-diameter SMA cables have been developed and characterized for structural engineering application. The authors conceptually came up with a novel SMA bracing system based on the SMA cables in previous study. To illustrate the feasibility of the SMA bracing system, further studies on the experimental verification of SMA brace's mechanical behavior and the numerical investigations for seismic performance assessment are conducted in this paper.

In particular, this paper discusses the mechanical response of a prototype SMA cable based bracing system and seismic performance of steel frame buildings with and without SMA bracing system. First, an SMA brace is designed and fabricated for experimental investigation. The mechanical behavior of the SMA brace is characterized through cyclic loading tests. Then, a numerical model of the SMA bracing system is developed in OpenSees. A four-story steel frame building with SMA bracing system is designed to have comparable strength and stiffness with a steel moment resisting frame (SMRF) as case-study building. A suit of 22 ground motions from FEMA P695 are selected and employed in numerical simulations. Nonlinear dynamic analyses are conducted to assess the efficiency of SMA bracing system for seismic response mitigation under DBE and MCE hazard levels. The seismic responses are analyzed and compared in terms of maximum interstory drift, maximum residual drift as well as maximum floor acceleration. The test results show that the SMA bracing system exhibits typical flag-shaped hysteretic behavior with good energy dissipation capacity and excellent self-centering capability. The numerical simulations reveal that the SMA bracing system can effectively enhance seismic performance of steel frame buildings at different hazard levels.

Keywords: SMA bracing system; SMA cables; Experimental study; Steel frame building; Seismic performance

1. Introduction

Shape memory alloys (SMAs), a class of smart metallic materials, are widely recognized and applied to achieve self-centering behavior in civil structures during the last two decades [1]. The SMA-based devices possess the extraordinary energy dissipation capacity and unique re-centering property such that they can efficiently reduce permanent residual deformations. Residual drifts are strongly correlated with post-event occupancy, structural reparability and economic losses [2-4]. For example, the FEMA P58 provisions defined the residual drift as an important index associated with structural damage states and economic feasibility of repair [5].

A number of SMA-based passive control device have been developed to decrease the residual drift and mitigate seismic response. Yang [6] came up with a cost-effective hybrid device by using mild steel struts and a set of SMA wires to maximize both energy dissipation and re-centering capabilities. Miller [7] experimentally investigated the behavior of a self-centering buckling-restrained brace, which is a typical buckling-restrained brace alongside of pre-tensioned NiTi SMA rods in parallel for generating self-centering force. Araki [8] presents a viable solution including cyclic tests of the behavior of superelastic Cu–Al–Mn SMA tension brace that consists of an SMA bar, a steel rod, and a stopper. Qiu [9] examined the performance and feasibility of SMA brace which is consist of two sliding blocks and two steel rods wrapped with two group NiTi SMA wires. The NiTi SMA wires are the kernel of the brace and enable the brace work effectively in both tension and compression. Recently, the large-diameter SMA cables, a relative new component composed of strands of wires, have been explored for the potential application in structural engineering [10-11]. The SMA material in cable form possesses both large-force capacity and superelastic characteristic. The authors conceptually proposed a novel SMA bracing system on the basis of SMA cables to enhance the seismic performance in a previous study [12-13].

This study examines the fabrication feasibility and experimental behavior of the proposed SMA bracing system and explored the seismic performance enhancement of steel frame building with the SMA bracing system. To this end, an SMA brace specimen is first designed and fabricated. Then, the mechanical behavior of SMA bracing system is investigated under cyclic loading test. Next, the nonlinear dynamic analyses are conducted for the four-story steel frame buildings with and without SMA bracing system.

2. SMA bracing system

2.1 SMA cables

The main component of the proposed SMA bracing system is SMA cable. The SMA cables utilized in this study are made of Nickel-Titanium (NiTi) and have an outer cable diameter of 8 mm. The cable consists of a total of 49 individual wires with a diameter of 0.885 mm. The wires are arranged in a 7 × 7 configuration, where each of seven wires composes a strand as shown in Fig. 1.

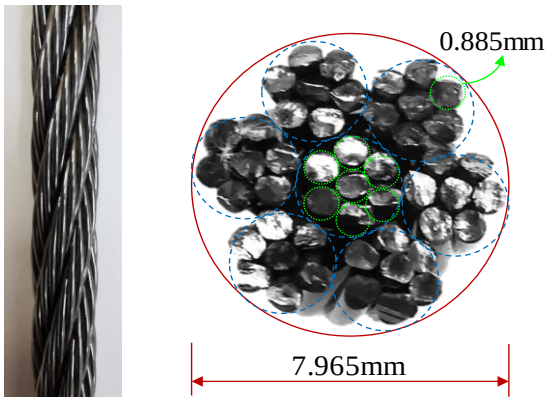

Fig. 1 Configuration of SMA cable

2.2. Design of SMA bracing system

In order to improve the performance of steel moment resisting frame, an SMA-based bracing system is manufactured and tested in this study. A schematic view and manufactured specimen of the SMA bracing system are shown in Fig. 2. The SMA bracing system consists of an outer member, an inner member, SMA tendons, two end plates, a connection plate and two guide members. The inner member is a steel I-section with an extended web at one end. The inner member is placed into the outer tubular member to guide the SMA cables. The outer member is a steel box section with a connection plate at one of its end. The SMA cables are anchored at both ends to the end steel plates that can freely move under the guidance of inner member.

The design mechanism of the SMA-based brace enables SMA cables to work in tension when the bracing system itself is either under tension or compression. When the SMA brace is under compression, the inner member moves to right and push the right end plate away. However, the left end plate is blocked by the outer member, which produces tensile forces in the SMA cables. When the bracing system is in tension, the inner member pulls the left end plate but the right end plate is blocked by two guide members attached to the outer box beam. Therefore, the SMA cables again experience tensile loads. This design mechanism enables the SMA cables to be effective whether the brace itself is under tension or compression.

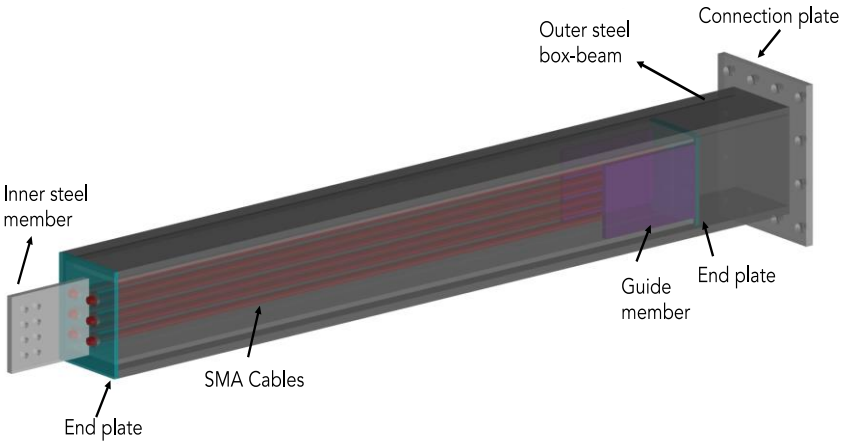

(a) schematic view of SMA bracing system

(b) SMA brace specimen

Fig. 2 SMA bracing system

3. Mechanical behavior of SMA brace

3.1 Loading protocol

An MTS actuator is used to apply various displacements to the SMA bracing system specimen. The test is conducted using cyclic loading protocol at ambient temperature. In order to explore the mechanical behavior

of SMA bracing system under different deformation amplitudes, the specimen is tested at six displacement levels that are 5 mm, 10 mm, 15 mm, 20 mm, 25 mm, and 30 mm. All tests are conducted at a loading frequency of 0.01 Hz for three loading cycles.

3.2 Experimental results

The third cycle for each loading displacement levels was applied to evaluate the mechanical behavior of SMA bracing system. Fig. 3 shows the force-displacement curves of SMA brace for all displacement levels. It can be seen that the SMA brace exhibits flag-shaped hysteretic curves with good energy dissipation capability and excellent self-centering characteristic.

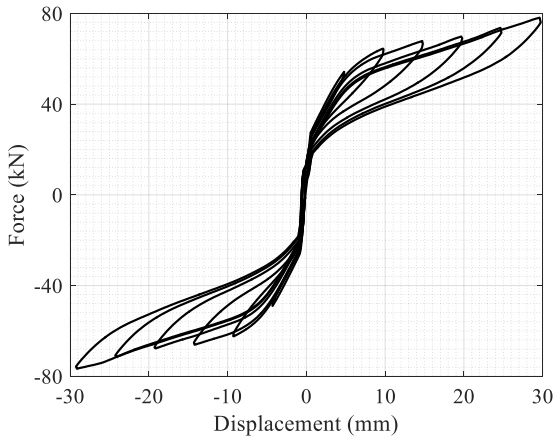

Fig. 3 Hysteretic curves of SMA brace at various displacements at loading frequency of 0.01Hz

To enable explore the mechanical properties of the SMA brace more quantitative, Fig.4 shows the variation of the maximum force, equivalent stiffness (K_{eqv}), dissipated energy (E_d), and equivalent viscous damping ratio (ξ_{eqv}) with the deformation amplitude. The maximum force and dissipated energy increase with the increasing of loading displacement, while the dissipated energy almost increased linearly. The equivalent stiffness decreases with the increasing of loading displacement, but the rate of this decrease reduces at larger displacement amplitude. The equivalent viscous damping ratio increases rapidly when the loading displacement increases from 5 mm to 15 mm, then remains almost constant at larger displacement amplitude. The value of equivalent viscous damping ratio varies from 2.28% to 5.53%, this indicates that the SMA brace can provide relatively a good energy dissipation capability.

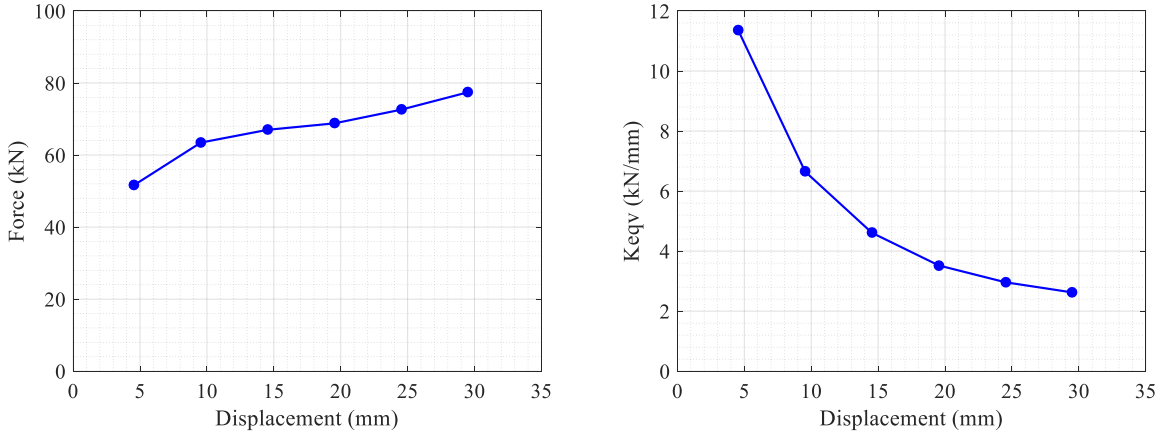

(a) (b)

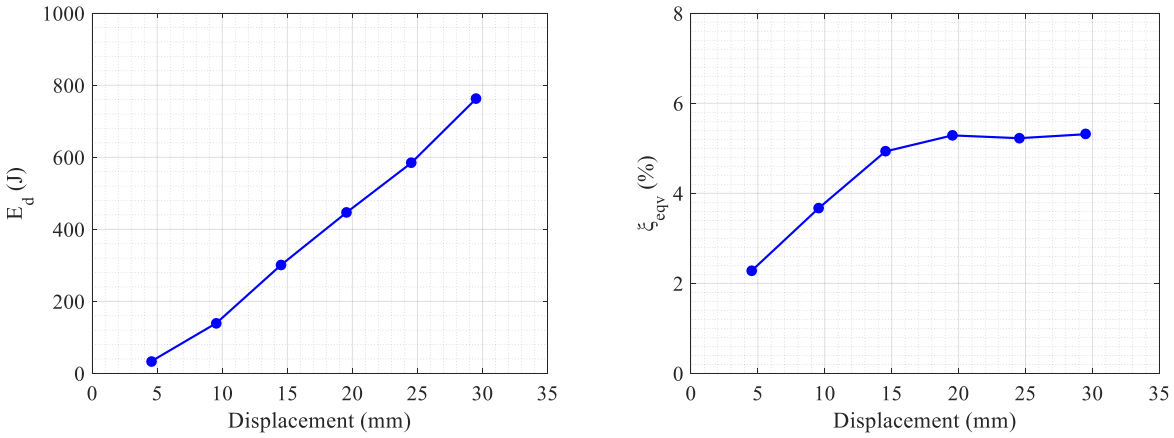

(c) (d)

Fig. 4 Variation of (a) the maximum force, (b) equivalent stiffness, (c) dissipated energy, and (d) equivalent viscous damping ratio with deformation amplitude.

4. Numerical investigations

4.1 Modeling of SMA bracing system

A numerical model is developed in OpenSEES to accurately simulate the behavior of SMA brace at various deformation levels [13]. The model consists of two self-centering materials in parallel with a multi-linear spring as shown in Fig 5(a). Two self-centering materials are mainly used to capture the flag-shape area of the hysteretic curve, while the multi-linear spring adjusts the stiffness of the entire mechanical model and enables smooth transition from initial response to the post-hardening region. The ultimate state of SMA cables is incorporated into the model by using a material object that defines zero stress when the SMA strains fall below or above a certain threshold value.

The SMA bracing system behavior relies on the mechanical response of SMA cables. Fig 5(b) shows the stress-strain curves of SMA cables at various loading strains and the predicted response for the proposed model. The parameters selected for self-centering and multi-linear springs to predict the hysteretic response of SMA cables are shown in Table 1. As can be seen from Figure 5(b), the developed model closely captures the behavior of SMA cables at different loading deformations.

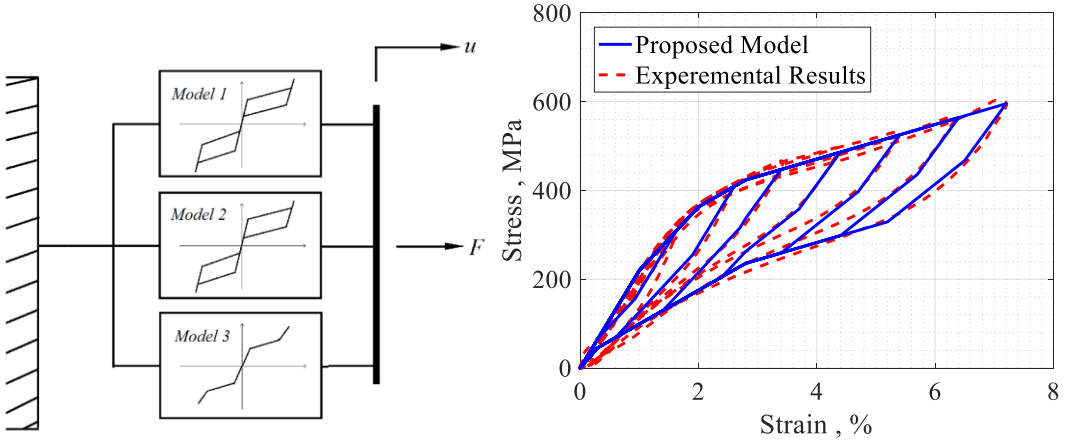

(a) (b)

Fig. 5 (a) Schematic representation of proposed model, and (b) proposed model prediction.

Table 1. Parameters for proposed SMA model

Parameters	Models		
	1	2	3
Initial stiffness (*MPa / %*)	80	90	50
Post-transformation stiffness (*MPa / %*)	13	13	13
Forward transformation stress (*MPa*)	160	90	140
Ratio of forward to reverse activation stress (β)	1.0	0.7	0.0

4.2 Case-study buildings

The case-study steel frame building selected for numerical simulations is designed as an office building located on soil type D in Los Angeles. The structural system consists of steel special moment resisting frame (SMRF) designed with fully restrained reduced beam sections and connected with partial restrained gravity frame. The building is designed in accordance with IBC (2003), SEI/ASCE-02 and ASIC (2002) design provisions. The plan and elevation of the East-West direction of the building are shown in Fig 6(b). The structure is classified as Category II and the Maximum Considered Earthquake (MCE) spectral response acceleration is 1.5g at short periods (SS) and 0.9g at 1 second period (S1). The design spectral acceleration parameters SMS and SM1 are 1.0g and 0.6g. More details of the case-study frame building can be found in Lignos[14].

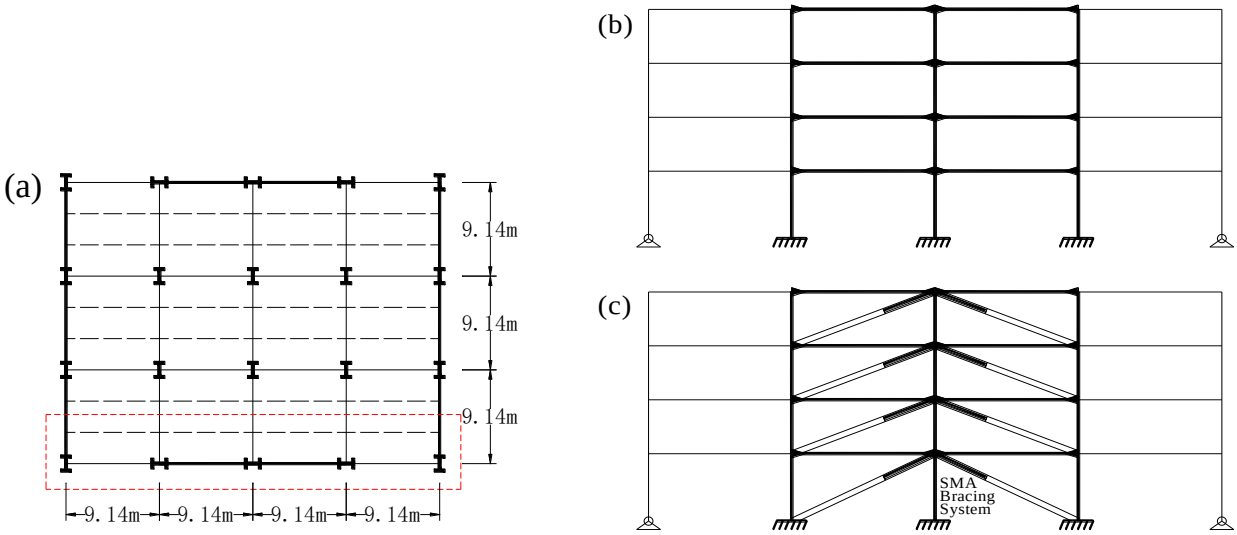

Fig. 6 Structural model illustration: (a) Plan view; East-West elevation of (b) SMRF and (c) SMA frame.

In addtion, an SMA-braced frame is designed such that it has comparable strength and stiffness with the original SMRF. To achieve this, the strength of the SMRF is reduced by selecting smaller beam and column section sizes for the frame system such that the reduced strength frame has a base shear capacity equal to about 75% of the base shear capacity of the original SMRF and the selected frame sections satisfy the strength requirements of ASCE 7-10 and ANSI/AISC 360-10. Then, the diagonal bracing configuration for SMA braces is adopted and SMA braces are installed at each bay at each story of moment resisting frame as shown in Fig 6(c). The area and length of the SMA cables utilized in this study are 600 mm^2 and 2000 mm for lower two stories, 350 mm^2 and 1700 mm for upper two stories, respectively.

4.3 Modeling strategy

The numerical models of the case-study frames are developed using the OpenSees platform. The beams and columns are modeled using two zero-length elements with rotational springs at the ends of the member and

an elastic beam-column element in the middle of the member. The nonlinear behavior of the plastic hinge rotational spring is represented by the modified Ibarra-Medina Krawinkler (IMK) model, which properly takes component strength deterioration, post-capping strength deterioration and unloading stiffness deterioration into account and is calibrated by more than 350 experimental data [15,16]. The panel zone is simulated following the approach described in ATC 72-1. A trilinear model without deterioration consideration proposed by Gupta and Krawinkler [17] is applied to capture the shear distortion hysteretic behavior of the panel zone. In addition, the P-delta effect associated with the interior gravity loads is considered in the analytical model utilizing an additional leaning column. The leaning column is modeled by rigid column elements connected by rotational springs with very small stiffness. Damping ratio equal to 3% is assigned to the building models. The built models for SMRF and SMA Frame have fundamental periods of 1.21s and 1.28s, respectively. More detail of the model parameters and calibration can be found in Shi [12].

4.4 Ground motions

A suite of 22 far field ground motions from FEMA P-695 [18] are adopted in this study to sufficiently consider the uncertainty associated with earthquake record variability. The magnitudes of the selected records range from M6.5 to M7.6, while the site-source distances ranges between 11.1 km and 26.4 km. Peak ground acceleration (PGA) and peak ground velocity (PGV) values vary from 0.21g to 0.82g and from 19 cm/s to 115 cm/s, respectively. The response spectra of the individual records as well as median, DBE level and MCE level spectra are shown in Fig.7.

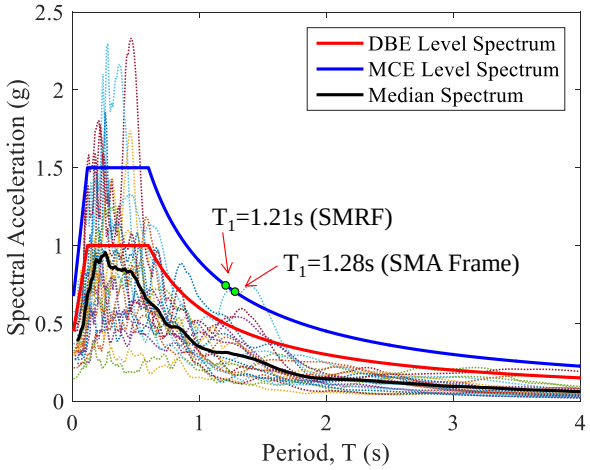

Fig. 7 Acceleration spectra of selected ground motions

4.5 Seismic performance

Nonlinear dynamic analysis is employed to assess the seismic performance of steel frame buildings under 22 ground motions. The responses of steel frame building with and without SMA bracing system are evaluated under two hazard levels corresponding to the design basis earthquake (DBE) level and the maximum considered earthquake (MCE) level.

Fig.8 illustrates the maximum interstory drift, residual drift and floor acceleration of SMA frame and SMRF under DBE and MCE hazard level 22 ground motions. It can be seen that the SMA frame has lower interstory drift demand for most cases at both DBE and MCE levels. There is one case for the SMRF where collapse was observed under ground motion 9 at MCE level. For the residual drift demand, the steel frame with SMA bracing system reduces the response considerably for almost all of the ground motion records. The median residual drift of all 22 ground motions is 0.28% and 0.63% for the SMA frame under DBE and MCE hazard level, respectively, while the residual drift of SMRF is 0.74% and 1.23%, respectively. For maximum floor acceleration, the SMA frame has comparable response with SMRF under both DBE and MCE levels.

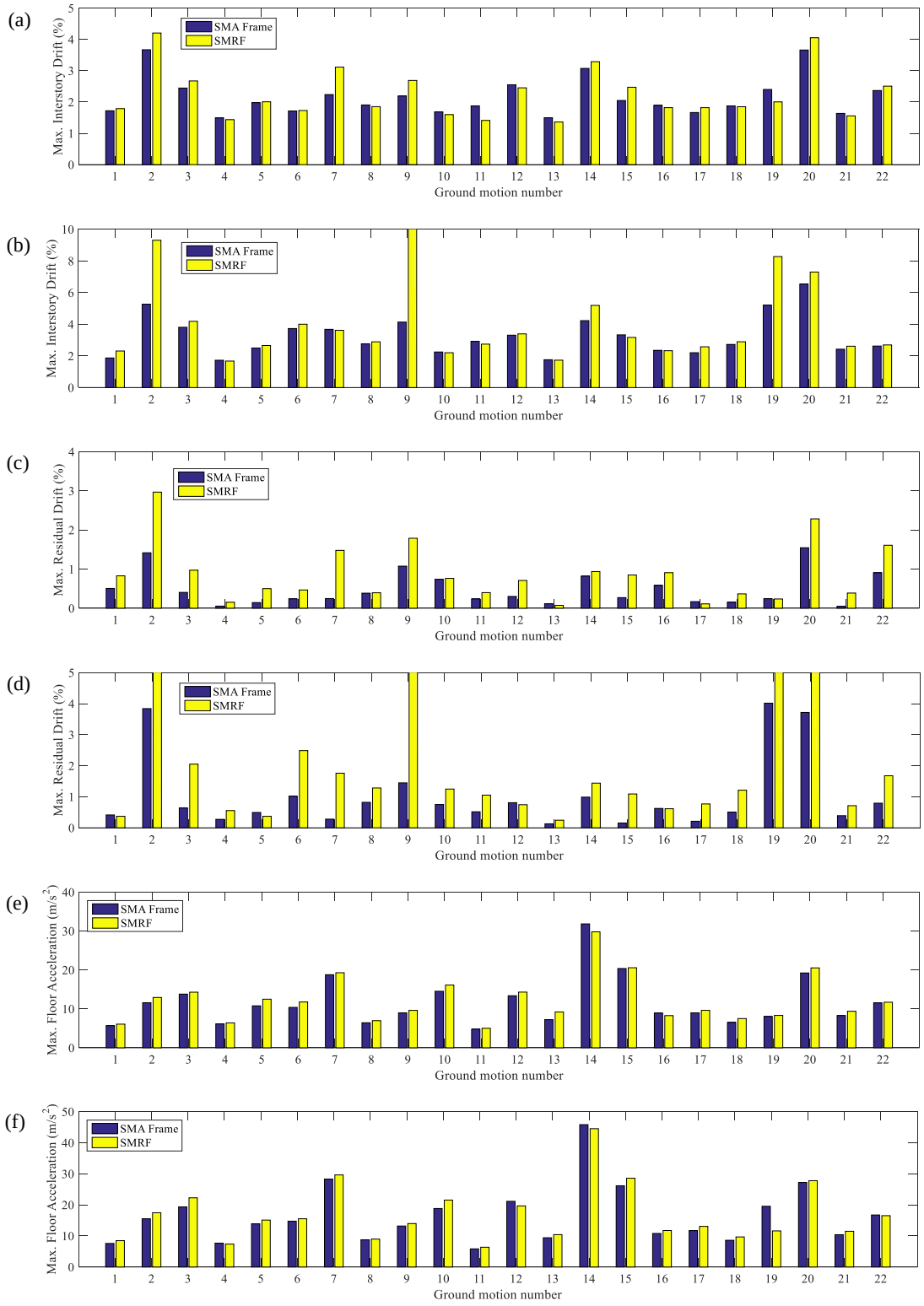

Fig. 8 Seismic response of max. Interstory drift, residual drift and floor acceleration of SMA frame and SMRF for 22 ground motions at (a), (c), (e) DBE and (b), (d), (f) MCE hazard levels.

To further elaborate on the efficacy of SMA bracing system in mitigating the seismic response, the base shear force versus first floor interstory drift curves for the SMA frame and SMRF subjected to Duzce earthquake are shown in Fig. 9. The final residual drift of the frames are highlighted with a solid circle in each case. It can be seen that the SMRF exhibits considerable residual deformation under both DBE and MCE hazard levels, while the SMA frame successfully limits the residual drifts although large nonlinear deformation experienced. Specifically, the residual drift response of SMA frame is 0.31% and 0.11%, whereas that of SMRF are 0.97% and 2.05% under DBE and MCE level, respectively.

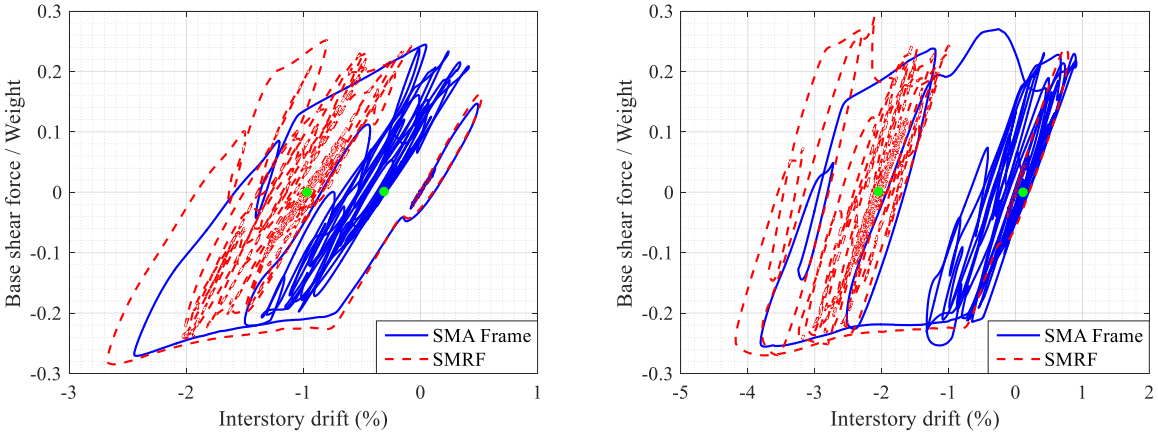

Fig. 9 Base shear versus first floor interstory drift response for the SMA frame and SMRF under Duzce earthquake scaled to (a) DBE and (b) MCE level.

5. Conclusions

In this study, the mechanical behavior and seismic performance enhancement of an SMA braced frame are examined. First, an SMA cable bracing system is designed and fabricated for experimental characterization. Cyclic loading tests are conducted for the SMA bracing system to characterize its mechanical response. A numerical model of the SMA bracing system that accurately predicts the behavior of SMA brace is developed. A four-story steel frame building is designed with and without the SMA bracing system and modeled in OpenSees. Nonlinear dynamic analysis is conducted under 22 far-field ground motions and maximum seismic responses are evaluated. The results show that the SMA brace system exhibits satisfactory flag-shaped hysteretic response with excellent self-centering capability. The residual drift demands of the steel frame buildings subjected to DBE and MCE level earthquakes can be substantially mitigated by equipping with SMA bracing system.

6. Acknowledgements

The research described in the paper was supported by the Natural Science Foundation of China under grant No.51878195.

7. References

[1] Ozbulut OE, Hurlebaus S, DesRoches R (2011): Seismic response control using shape memory alloys: a review. *Journal of Intelligent Material Systems and Structures*, **22**(14):1531-1549.

[2] Parulekar, YM, Reddy, GR, Vaze, KK, et al. (201w): Seismic response attenuation of structures using shape memory alloy dampers. *Structural control and health monitoring*, **19** (1): 102-119.

[3] Casciati F, Faravelli L, Al Saleh R. (2009): An SMA passive device proposed within the highway bridge benchmark. *Structural Control and Health Monitoring*, **16**(6), 657-667.

[4] Silwal B, Ozbulut OE, Michael RJ. (2016): Seismic collapse evaluation of steel moment resisting frames with superelastic viscous damper. *Journal of Constructional Steel Research*, **126**: 26-36.

[5] FEMA P-58. (2012): Seismic performance assessment of buildings. *Federal Emergency Management Agency*.

[6] Yang CW, DesRoches R, Leon RT. (2010): Design and analysis of braced frames with shape memory alloy and energy-absorbing hybrid devices. *Engineering Structures*, **32**:498-507.

[7] Miller DJ, Fahnestock LA, Eatherton MR. (2012): Development and experimental validation of a nickel–titanium shape memory alloy self-centering buckling-restrained brace. *Engineering Structures*, **40**:288-298.

[8] Araki Y, Shrestha1 KC, Maekawa N, Koetaka1 Y, Omori T, Kainuma R. (2016): Shaking table tests of steel frame with superelastic Cu-Al-Mn SMA tension braces. *Earthquake Engineering and Structural Dynamics*, **45**:297-314.

[9] Qiu C, Zhu S. (2017) Shake table test and numerical study of self-centering steel frame with SMA braces. *Earthquake Engineering and Structural Dynamics*, **46**(1):117-137.

[10] Ozbulut OE, Daghash S, Sherif MM. (2016): Shape Memory Alloy Cables for Structural Applications. *Journal of Materials in Civil Engineering*, **28**(4): 04015176.

[11] Fang C, Zheng Y, Chen J, Yam MCH, Wang W. (2019): Superelastic NiTi SMA cables: Thermal-mechanical behavior, hysteretic modeling and seismic application. *Engineering Structures*, **183**:533-549.

[12] Shi F, Saygili G, Ozbulut OE. (2018):Probabilistic seismic performance evaluation of SMA-braced steel frames considering SMA brace failure. *Bulletin of Earthquake Engineering*, **16**(12):5937-5962.

[13] Shi F, Ozbulut OE, Zhou Y. (2020): Influence of SMA Brace Design Parameters on Seismic and Collapse Performance of Self-Centering Steel Frame Buildings. *Structural control & Health Monitoring*, **27**(1): e2462.

[14] Lignos DG, Krawinkler H. (2012): Sidesway collapse of deteriorating structural systems under seismic excitations. *Rep.No. TB 177*. The John A. Blume Earthquake Engineering Research Center, Stanford University, Stanford, CA.

[15] Ibarra LF, Medina RA, Krawinkler H. (2005): Hysteretic models that incorporate strength and stiffness deterioration. *Earthquake Engineering and Structural Dynamics*, **34**(12):1489 -1511.

[16] Lignos DG, Krawinkler H. (2011): Deterioration modeling of steel components in support of collapse prediction of steel moment frames under earthquake loading. *Journal of Structural Engineering*, **137**(11):1291-1302.

[17] Gupta A, Krawinkler H. (1999): Seismic Demands for Performance Evaluation of Steel Moment Resisting Frame Structures. *Technical Report 132*. The John A. Blume Earthquake Engineering Research Center, Department of Civil Engineering, Stanford University, Stanford, CA.

[18] FEMA P695. (2009): Quantification of Building Seismic Performance Factors. Washington, D.C: *Federal Emergency Management Agency*.

